J Mater Sci (2010) 45:182–187
DOI 10.1007/s10853-009-3914-9

Surfactant-assisted fabrication of MoS_2 nanospheres

Zhuangzhi Wu · Dezhi Wang · Aokui Sun

Received: 20 May 2009 / Accepted: 19 September 2009 / Published online: 1 October 2009

Abstract The fabrication of MoS_2 nanospheres with an average diameter of 100 nm via a surfactant-assisted route was reported, in which an amorphous MoS_3 precursor was obtained by the aggregation transformation of surfactant at a low temperature and then transformed to the MoS_2 nanospheres with quasi-fullerene structures by thermal decomposition. The final products were characterized by XRD, IR, SEM, and TEM, respectively. The results indicate that the polyethylene glycol (PEG) promotes the formation of nanospheres and has a great effect on the microstructures, resulting in the abnormal expansion of lattice. The possible transformation mechanism of structures has been discussed based on the experimental results.

Introduction

There has been considerable interest in the transition metal dichalcogenide layered compounds, a group of anisotropic materials with strong bonding within the layers and weak interlayer interactions [1]. As one of the members of this family, MoS_2 has numerous applications as hydrodesulfurization catalyst [2], lubricant [3], super shock absorber [4], and intercalation host to form new materials [5].

To date, there are many methods which have been reported to synthesize MoS_2, for instance, gas-phase reactions [6], laser ablation [7], sonochemical process [8], hydrothermal synthesis [9, 10], thermal decomposition [11], etc. Among these approaches above, there are many kinds of micro/nano materials with various structures and morphologies, such as inorganic fullerene, nanotubes, nanorods, nanowires, microspheres, hollow spheres, etc.

While, only the fullerene-like and spherical structures have been proved that they can greatly improve lubrication properties of MoS_2 because of the rolling mechanism [3, 10]. The sliding and rolling frictions exist simultaneously between the friction pairs to make the anti-wear and friction-reducing properties much better. As a result, recently, many efforts have been made to prepare these structures. Du et al. [12] adopted a novel method to synthesize IF-MoS_2 with particle size of 10–20 nm. Chang et al. [13] obtained MoS_2 inorganic fullerene-like nanomaterials from MoS_2 amorphous nanoparticles by calcination. Huang et al. [14] prepared MoS_2 microspheres by the inducing of tungsten acid. Luo et al. [15] synthesized hollow MoS_2 microspheres with diameter of 2 μm in ionic liquids/water binary emulsions. Wu et al. [16] obtained MoS_2 microspheres with diameter of 0.5–2 μm by solvothermal method with addition of homemade surfactant SUDEI.

In our present study, a surfactant-assisted route was developed to fabricate MoS_2 nanospheres with an average diameter of 100 nm. In detail, the amorphous MoS_3 precursor was realized by the aggregation transformation of surfactant at a low temperature firstly and then transformed to the MoS_2 nanospheres by calcination.

Experimental

In a typical synthesis, 0.85 g $(NH_4)_2Mo_2O_7$ and 3.06 g $Na_2S{\cdot}9H_2O$ were dissolved in 100 mL distilled water to make solution A. A total of 2.88 g polyethylene glycol (PEG) with molecular weight of 20000 was dissolved in 100 mL distilled water to form solution B. Then, excessive

Z. Wu · D. Wang (✉) · A. Sun
School of Materials Science and Engineering,
Central South University, Changsha, Hunan 410083,
People's Republic of China
e-mail: dzwang@mail.csu.edu.cn; dzwang68@gmail.com

hydrochloric acid was added into the mixed solution of A and B with high-speed stirring for several minutes. The precipitate was filtered off, washed with ammonia, absolute ethanol, and distilled water for several times, and then dried in vacuum at 50 °C for 6 h. Finally, the as-prepared MoS_3 sample was annealed in a tubular furnace for 0.5 h at elevated temperatures from 400 to 800 °C in an atmosphere of H_2 to produce MoS_2.

X-ray diffraction (XRD) analysis was performed on a D/max-2500 diffractometer with CuKα radiation ($\lambda = 0.154$). FT-IR spectra were recorded on an Avatav 360 infrared spectrometer in the range of 500–4000 cm^{-1} using KBr pellets. SEM images were obtained using a FEI Sirion200. TEM images were obtained with a Tecnai G^2 20, operating with an accelerating voltage of 200 KV.

Results and discussion

XRD pattern reveals the poor-crystalline characteristics of the as-obtained sample before annealing treatment, which makes it difficult to identify its phase. The composition of the as-obtained sample is determined by the energy dispersive X-ray analysis (EDAX) and elemental analysis, showing that the product is composed of Mo, S with a mole ratio of 1:3.3 and an amount of C, O (the EDAX spectrum is not shown here). It is evident that the sample contains a lot of PEG. Figure 1 shows the IR spectra of PEG (a) and the as-obtained MoS_3 precursor (b). In Fig. 1a, the absorption peaks at 2888 and 1100 cm^{-1} are attributed to the stretched vibration of $–CH_2$ and C–O, respectively. The absorption peaks at 950 and 841 cm^{-1} are attributed to the splitting of $–CH_2$ [17]. The typical peaks of PEG also exist in Fig. 1b, indicating that an amount of PEG is adsorbed onto the surface of the MoS_3 nanospheres to form modification layers and cannot be washed off totally by ethanol and water.

Figure 2 shows the XRD patterns of the amorphous precursor and final products synthesized at different annealing temperatures. Compared with the wide and weak peak of the amorphous MoS_3 precursor (Fig. 2a), more peaks appear and become sharper with the temperature increasing from 400 to 800 °C, and the peak intensity increases rapidly. The above results indicate that the structures become more integrated and 2H-MoS_2 with characteristic peaks of (002), (100), (103), and (110) appears at the annealing temperature of 800 °C (indexing JCPDS file No. 37-1492). The (002) peaks of these annealed samples are characterized by a shift to lower angles as compared to the (002) peak in hexagonal 2H-MoS_2 crystal. The shift in the (002) peaks indicates lattice expansion about 9% (Fig. 2b), 6% (Fig. 2c) and 2% (Fig. 2d) along the *c*-axis at different annealing temperatures, for the introduction of crystal defects or strains owing to curvature of the layers [6, 18, 19].

Figure 3 shows the morphologies of the as-prepared MoS_2 annealed at 800 °C for 0.5 h in an atmosphere of H_2. These SEM images suggest that the MoS_2 nanospheres are obtained with an average diameter of 100 nm on a large scale. The TEM images in Fig. 4 reveal the dramatic changes from the amorphous MoS_3 precursor to the final MoS_2 product following the heat treatment. After annealed at 400 °C, the PEG combined with MoS_2 begins to evaporate, and the perfect surface becomes rough. Up to

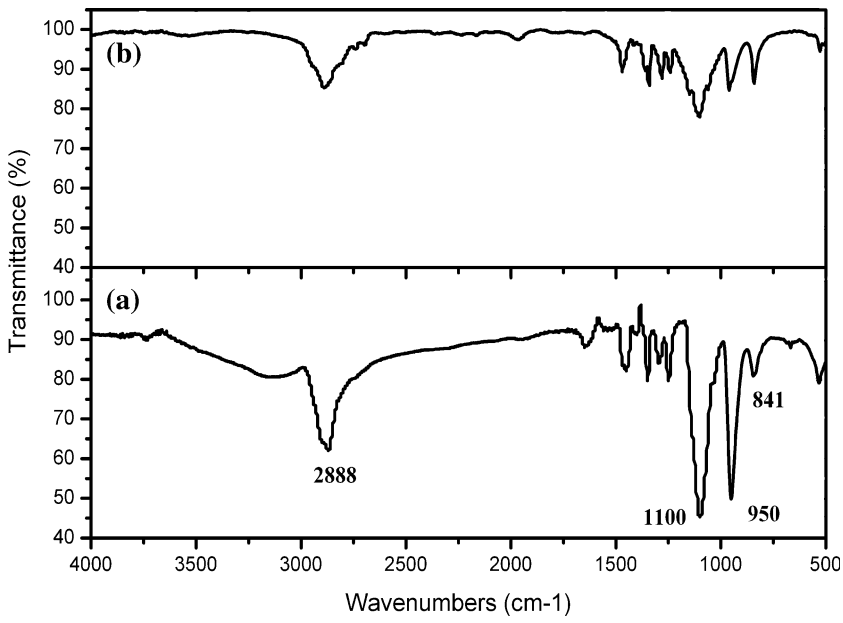

Fig. 1 IR spectra of PEG (**a**) and the MoS_3 nanospheres (**b**)

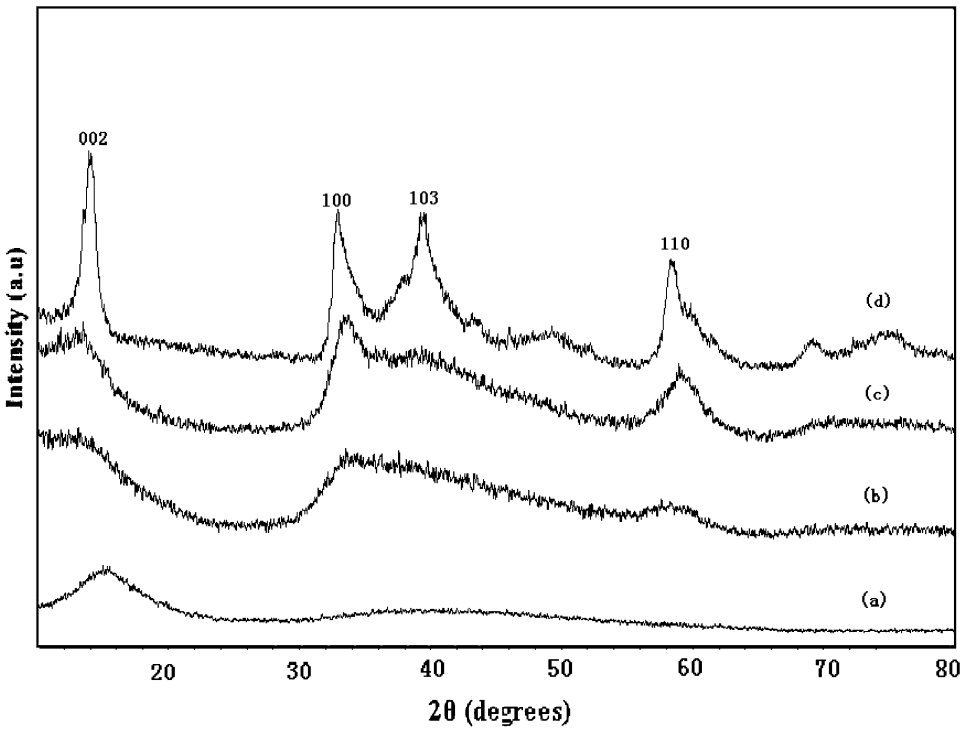

Fig. 2 XRD patterns of (*a*) the amorphous MoS_3 precursor and samples annealed at different temperatures: (*b*) 400 °C; (*c*) 600 °C; and (*d*) 800 °C

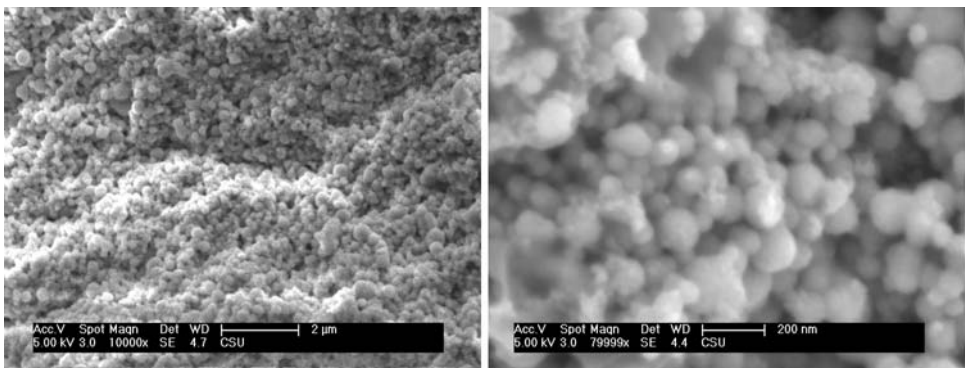

Fig. 3 SEM images of the MoS_2 nanospheres obtained by calcination at 800 °C for 0.5 h in H_2

600 °C, as shown in Fig. 4b, the evaporation and exfoliation are enhanced. With the temperature increased to 800 °C, almost all the PEG exfoliates away from MoS_2. Due to the disappearance of the binding effect of PEG, the microstructures become looser and the volume of the nanospheres expands largely, as shown in Fig. 4d.

To investigate the effect of PEG on the microstructures, the TEM images of the precursor and final products with high magnification are shown in Fig. 5. There are no significantly special structures in the amorphous MoS_3 precursor, but the adsorbed layer of PEG can be found on the edge, as shown in Fig. 5a. After annealing treatment, the MoS_3 precursor turns into MoS_2 by thermal decomposition, and there are typical lamellar structures observed in the product of MoS_2, as shown in Figs. 5b–e. Obviously, higher temperature is helpful in crystallization of the product. The calcination at low temperature (400 °C) leads to low stacking and high disorder which are indicated by the wide (002) peak in Fig. 2b. With the temperature increased to 600 °C, the crystallization is improved and lamellar structures are well-stacked with short fringes. While, the carbonaceous matter will prevent the crystallization of MoS_2, leading to the decrease of layer stacking and textural stabilization [20], so the crystallization of MoS_2 modified by PEG is worse, compared to those without modification [13].

Furthermore, because of the binding effect of PEG, the sulfur can not be released completely, and it is adsorbed on the layers to stabilize them as the product of thermal decomposition [21]. As a result, corresponding to the XRD pattern, the interlayer distance is abnormally enlarged to 0.671 nm (annealed at 400 °C) because of the intercalation

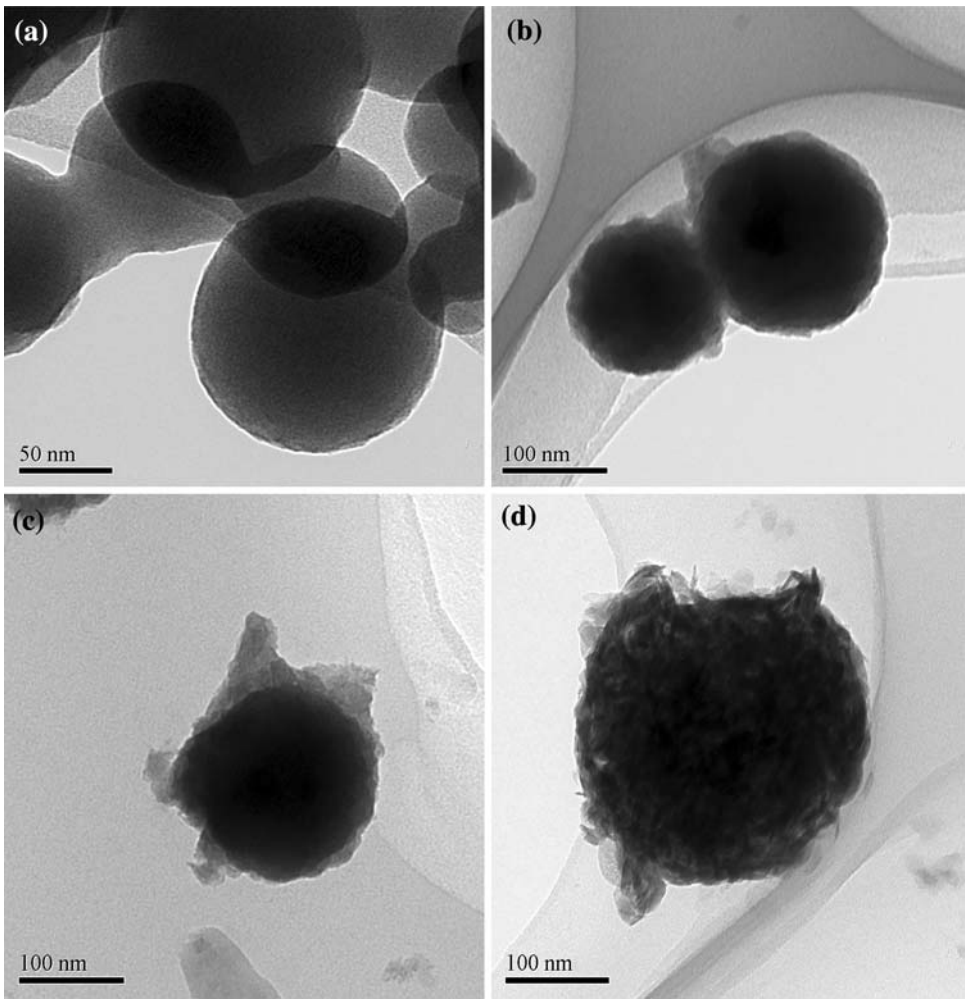

Fig. 4 TEM images for the amorphous MoS_3 (**a**) and as-obtained MoS_2 products annealed at different temperatures: (**b**) 400 °C, (**c**) 600 °C, and (**d**) 800 °C

of sulfur, indicating that the lattice expansion is up to 9%. Higher annealing temperature (600 °C) weakens the binding effect of PEG and part of sulfur is released slowly from the interlayer. Thus, the interlayer distance and lattice expansion are reduced to 0.653 nm and 6%, respectively. At higher annealing temperature (800 °C), the PEG and sulfur are removed completely and the volume of the nanospheres is enlarged significantly because of the disappearance of the binding effect of PEG. Driven by thermal energy, the lamellar structures are well-stacked with long fringes and quasi-fullerene structures are also observed, as shown in Fig. 5e. Moreover, the interlayer distance is 0.628 nm with lattice expansion of 2%, which is consistent with the report of Tenne et al. [18], attributed to the curvature of layers.

Finally, it must be noted that the PEG plays a crucial role in the formation of nanospheres because of the binding effect. And the unique morphology of nanospheres may be applied as accession to enhance lubricating performance and offer potential applications in the field of tribology. The present surfactant-assisted route is easy to control over all the reaction process and the simple fabrication with low cost may offer an alternative route to synthesize other advanced nanomaterials.

Conclusions

MoS_2 nanospheres with an average diameter of 100 nm have been synthesized successfully via a surfactant-assisted route, in which amorphous MoS_3 nanospheres are driven by the aggregation transformation of surfactant at a low temperature and then transformed to the MoS_2 nanospheres with quasi-fullerene structures by high-temperature calcination. The PEG not only promotes the formation of nanospheres by the binding effect, but also prevents the crystallization of MoS_2, leading to the decrease of layer stacking and textural stabilization. Furthermore, the binding effect of PEG prevents the complete release of sulfur, resulting in the abnormal expansion of lattice and interlayer distance. Moreover, the special morphology of nanospheres will be paid more attention in the exploration

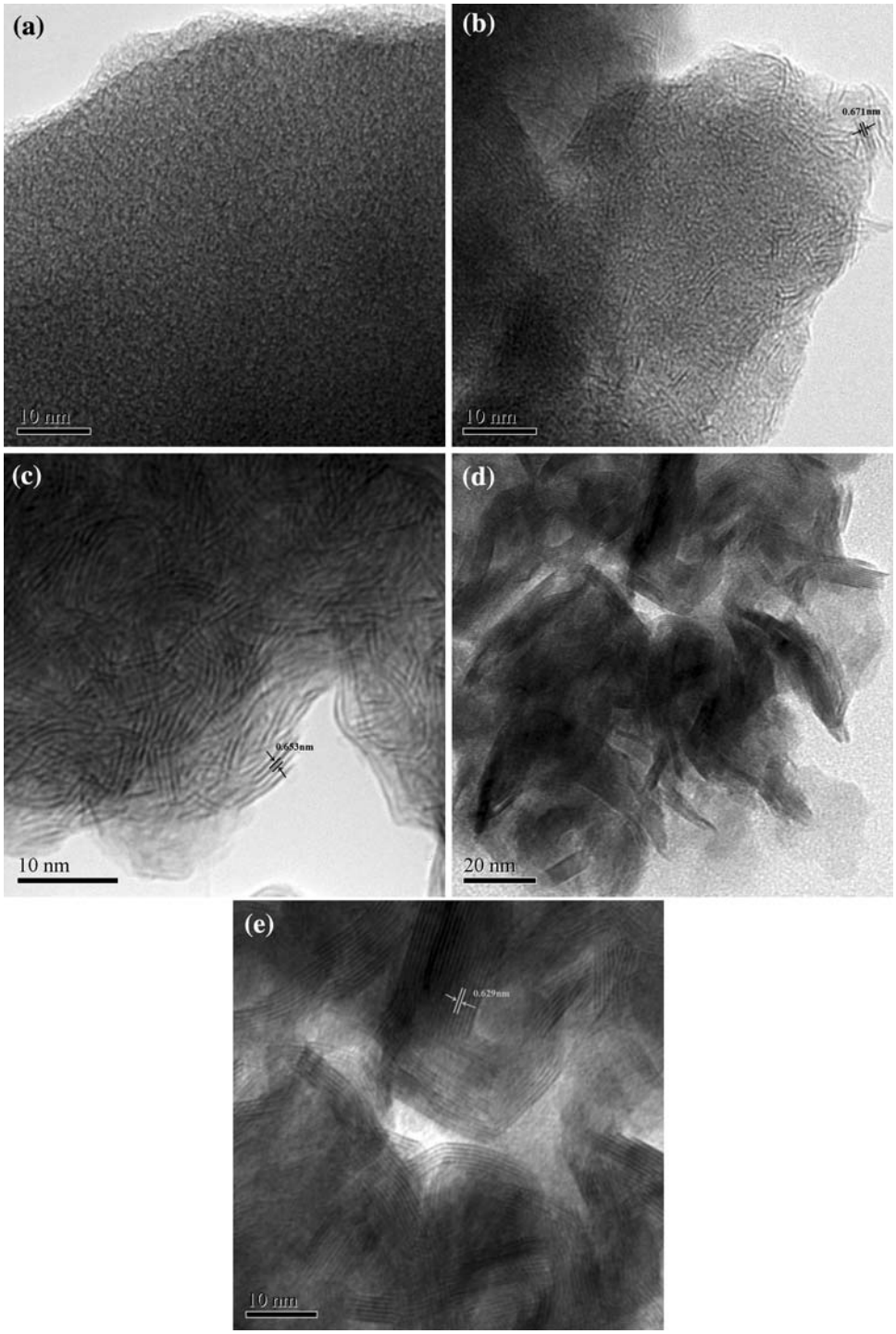

Fig. 5 TEM images with high magnification of the amorphous MoS_3 (**a**) and as-obtained MoS_2 products annealed at different temperatures: (**b**) 400 °C, (**c**) 600 °C, (**d**) 800 °C, and (**e**) enlarged image of (**d**)

of high effective lubricants due to the unique rolling mechanism.

References

1. Chianelli RR, Prestridge EB, Pecoraro TA, DeNeufville JP (1979) Science 203:1105
2. Chen J, Li S, Xu Q, Tanaka K (2002) Chem Commun 1722
3. Wang J, Zhao WZ, Guo CW (2009) J Mater Sci 44:227. doi: 10.1007/s10853-008-3082-3
4. Zhu YQ, Sekine T, Li YH, Wang WX, Fay MW, Edwards H, Brown PD, Fleischer N, Tenne R (2005) Adv Mater 17:1500
5. Winter M, Besenhard JQ, Spahr ME, Novak P (1998) Adv Mater 10:725
6. Feldman Y, Wasserman E, Srolovitz DJ, Tenne R (1995) Science 267:222
7. Parilla PA, Dillon AC, Jones KM, Riker G, Schulz DL, Ginley DS, Heben MJ (1999) Nature 397:114

8. Zheng XW, Zhu LY, Yan AH, Bai CN, Xie Y (2004) Ultrason Sonochem 11:83
9. Li WJ, Shi EW, Ko J, Chen ZZ, Ogino H, Fukuda T (2003) J Cryst Growth 250:418
10. Shi HQ, Fu X, Zhou XD, Wang DB, Hu ZS (2006) J Solid State Chem 179:1690
11. Nath M, Govindaraj A, Rao CN (2001) Adv Mater 13:283
12. Du K, Fu WY, Wei RH, Yang HB, Liu SK, Liu SD, Yu SD, Zou GT (2007) Mater Lett 61:4887
13. Chang LX, Yang HB, Fu WY, Zhang JZ, Yu QJ, Zhu HY, Chen JJ, Wei RH, Sui YM, Pang XF, Zou GT (2008) Mater Res Bull 43:2427
14. Huang WZ, Xu ZD, Liu R, Ye XF, Zheng YF (2008) Mater Res Bull 43:2799
15. Luo H, Xu C, Zou DB, Wang L, Ying TK (2008) Mater Lett 62:3558
16. Wu DM, Zhou XD, Fu X, Shi HQ, Wang DB, Hu ZS (2006) J Mater Sci 41:5682. doi:10.1007/s10853-006-0245-y
17. Wu ZZ, Wang DZ, Xu B (2008) Acta Phys-Chim Sin 24:1927 (In Chinese)
18. Srolovitz DJ, Safran SA, Homyonfer M, Tenne R (1995) Phys Rev Lett 74:1779
19. Berdinsky AS, Chadderton LT, Yoo JB, Gutakovsky AK, Fedorov VE, Mazalov LN, Fink D (2005) Appl Phys A 80:61
20. Afanasiev P, Xia G, Berhault G, Jouguet B, Lacroix M (1999) Chem Mater 11:3216
21. Peng YY, Meng ZY, Zhong C, Lu J, Yu WC, Yang ZP, Qian YT (2001) J Solid State Chem 159:170